MULTIOBJECTIVE DYNAMIC APERTURE OPTIMIZATION AT NSLS-II*

L. Yang†, Y. Li, W. Guo, S. Krinsky
Brookhaven National Laboratory, Upton, NY 11973

Abstract

In this paper we present a multiobjective approach to the dynamic aperture (DA) optimization. Taking the NSLS-II lattice as an example, we have used both sextupoles and quadrupoles as tuning variables to optimize both on-momentum and off-momentum DA. The geometric and chromatic sextupoles are used for nonlinear properties while the tunes are independently varied by quadrupoles. The dispersion and emittance are fixed during tunes variation. The algorithms, procedures, performances and results of our optimization of DA will be discussed and they are found to be robust, general and easy to apply to similar problems.

INTRODUCTION

Dynamic Aperture (DA) is one of the key nonlinear properties for a storage ring. Although there have been numerical tools to find the aperture, the reverse problem of how to optimize it is still a challenging problem. One approach of minimizing nonlinear driving terms has been applied to the lattice of National Synchrotron Light Source II (NSLS-II) storage ring [1, 5]. Recently, an alternative approach of using Multiobjective Evolutionary Algorithm (MOEA) [7, 6, 8, 3, 4] is developed. In the following sections we will take NSLS-II lattice as an example to discuss the procedures and results of this new approach to DA optimization.

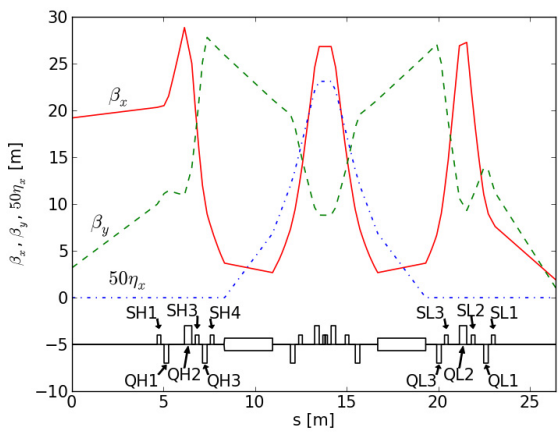

Figure 1: Lattice functions and magnet layout of one DBA cell.

NSLS-II is a state-of-the-art third-generation light source under construction at Brookhaven National Laboratory (BNL) [2]. The lattice has 30 double bend achromatic (DBA) cells. Each DBA cell has low and high beta functions at each side, with a short and long straight section respectively. Every nearby two DBA cells have mirror symmetry about the center of the straight section (see Fig. 1). The whole bare lattice has 15-fold symmetry. Each DBA cell has nine sextupoles, three sitting in between the dipoles have non-zero dispersion and are used for adjusting chromaticities. The other six, three on each side, are at the non-dispersive straight section. Three damping wigglers are included in the 2nd, 7th and 12th long straight sections but the 3-fold linear lattice is matched to be approximately 15-fold symmetric.

OBJECTIVE FUNCTIONS AND CONSTRAINTS

Instead of starting from a single initial solution, MOEA is applied to a set of candidate solutions iteratively. Each iteration is called one generation. At the first step, a fixed number of candidates are initialized as the first generation, and in our case they are uniformly distributed in parameter space $[x_1^L, x_1^U] \times [x_2^L, x_2^U] \times \cdots \times [x_N^L, x_N^U]$. Then one pair of them is randomly chosen as parents to generate two new children. This process is called cross-over and is repeated until the population is doubled. The third step is called mutation, where new children are perturbed slightly. The objective functions $f_i(\mathbf{x})$, constraints $g_j(\mathbf{x})$ are evaluated for each of these new children. The whole population, including the parents, is then sorted or ranked according to their dominance relations (see [6, 8] for dominance). Candidates not dominated by anyone are in the first rank. The second rank candidates are only dominated by the rank-one candidates, and the third ranks are only dominated by the first and second ranks, etc. The final step is a population control process, where only half of the better candidates are kept. This is done by dropping candidates with larger rank. Within same rank, candidates in a high population density region have lower priority to be kept. This is called one generation or one iteration. The population is evolved generation by generation until it converges or reaches the maximum number of iterations.

The DA used for objective function in our optimization is from direct tracking and it is a measure of survival particles after certain turns of tracking. Given initial (x, y, δ), the particles are tracked in a ring where various kinds of errors are included, e.g. misalignment, multipole errors. The objective functions of DA optimization are geometries of DA at different momentum and are quantified by their area

* work supported by DOE contract DE-AC02-98CH10886
† lyyang@bnl.gov

and an interior ellipse (in x–y plane) they must cover (See Fig. 2). The DA area is the number to maximize and covering the interior ellipse is the constraints of optimizations.

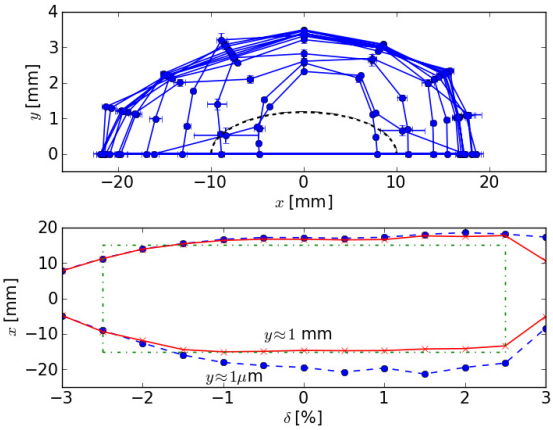

Figure 2: Examples of dynamic aperture in x–y plane (top) for 13 uniformly distributed $\delta \in [-3\%, 3\%]$ and δ–x plane (bottom) for $y = 1\mu m$ and $y = 1\ mm$. The dashed lines in each subplot are the constraints.

As shown in the top figure of Fig. 2, the objective functions and constraints for x–y plane are

$$\begin{cases} f_1 = S(\delta = 0) \\ f_2 = S(\delta = -2.5\%) + S(\delta = 2.5\%) \\ g_k = \frac{x_i^2(\delta_k)}{A_x^2} + \frac{y_i^2(\delta_k)}{A_y^2} - 1 \geq 0 \end{cases} \quad (1)$$

where f_1 the DA area of $\delta = 0$, f_2 the average of DA area of $\delta = \pm 2.5\%$, g_k the constraints for DA at $\delta_k = -2.5\%, 0, 2.5\%$ $(k = 1, 2, 3)$ and A_x, A_y the axes of constraint ellipse. $g_k \geq 0$ are set to optimize the overall shape of the DA instead of area alone. A similar setting which emphasize the δ–x plane can be setup as the following:

$$\begin{cases} f_1 = \sum_\delta S(\delta, y = 1\mu m) \quad (\delta \in [-3\%, 3\%]) \\ f_2 = 1/\left[\left(\frac{\partial \nu_x}{\partial J_x}\right)^2 + \left(\frac{\partial \nu_x}{\partial J_y}\right)^2 + \left(\frac{\partial \nu_y}{\partial J_y}\right)^2\right] \\ g_{p,i} = x_{p,i}(\delta_i) - A_{x,p} \geq 0 \\ g_{n,i} = x_{n,i}(\delta_i) - A_{x,n} \geq 0 \end{cases} \quad (2)$$

where f_1 the area of DA in δ–x plane at a fixed vertical offset $y = 1\mu m$, f_2 inverse of a sum of the squared tune-shift-with-amplitude terms, $g_{p,i}$ and $g_{n,i}$ the constraints for DA at positive and negative x axis, $x_{p,i}$ and $x_{n,i}$ DA positive and negative boundary of x at δ_i, $A_{x,p}$ and $A_{x,n}$ the positive and negative boundary of constraint rectangle for x (see bottom plot of Fig. 2). In our applications, the second approach in Eq. 2 is more fast in tracking and convergence, and will be discussed in the following.

INDEPENDENT VARIABLES

The independent variables for DA optimization are mainly sextupoles. There are six in the non-dispersive straight sections and three in the dispersive regions between dipoles. In our applications, the chromaticities are fixed and two sextupoles in-between dipoles are used for this purpose. The third sextupole in this dispersive region is a knob for the higher order chromaticities.

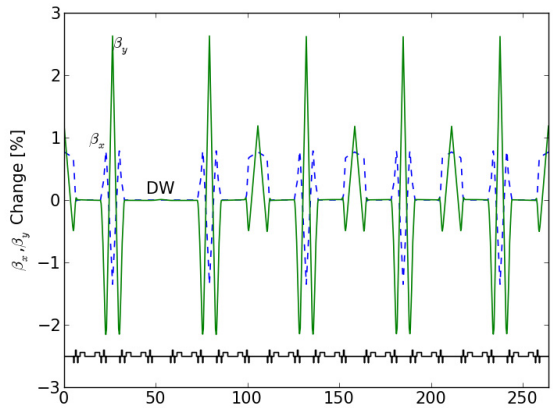

Figure 3: Beta function variation resulting from tunes change from $(33.15, 16.27)$ to $(33.16, 16.23)$. Changes in short and long straight are independent, and the damping wiggler section is not changed. In each DBA cell, linear lattice between dipoles is not changed.

The tunes are also allowed to change in certain range in the optimization by varying the quadrupoles. Given the example lattice with tunes $(33.15, 16.27)$, three quadrupoles, at each side of the straight section (QH1, QH2, QH3 at the high beta region and QL1, QL2, QL3 at the low beta region), are used to change the working point and keep the twiss function between dipoles fixed. As shown in Fig. 3, the twiss functions in non-dispersive regions do not change as we move working point from $(33.15, 16.27)$ to $(33.16, 16.23)$. The beta functions of the 2nd, 7th and 12th long straight sections where damping wigglers sit did not change either.

OPTIMIZATION AND RESULTS

The optimizations are carried out on about 180 2.33 GHz Xeon CPUs of a Sun Grid Engine (SGE) cluster and the underlying tracking of DA in our optimization uses a symplectic tracking code called TESLA [9]. It applies multi-particle tracking to speed up DA searching and parallelization of MOEA to speed up the optimizer.

The DA is tune dependent, but with the method of minimizing driving terms, we can not include tune as a variable. Because each of the driving terms is tune and beta functions dependent, there is no meaning to comparing the absolute values of a single driving term of different tunes or lattices.

DA from Direct tracking can overcome this problem and explore in a wider range of working points.

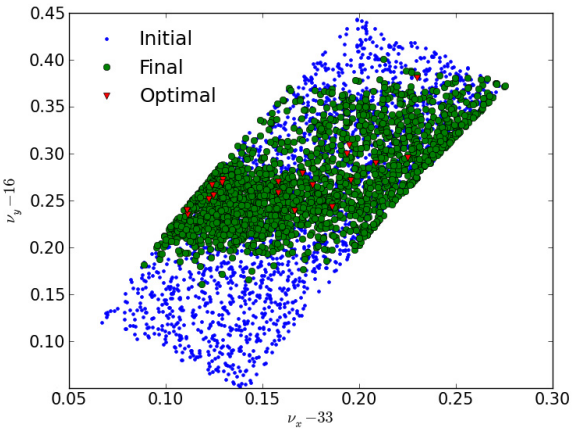

Figure 4: The tune variation range when matching long and short straight sections independently. The blue dots are initial tune coverage of the first generation. The green circles are from the final population, and red triangles are optimal candidates. All lattice are at chromaticity $(5, 5)$.

Fig. 4 shows the tune range of an optimization. The blue dots are the initial tunes from perturbations of lattice with tunes $(33.15, 16.27)$. As the quadrupole strength are perturbed uniformly, the tunes distribution covers a regular range bounded by integer and half integer. As the optimization proceeds, the final population has tunes distributed as green circles ($\nu_y \in [16.15, 16.40]$). Because of the high chromaticity, $(5, 5)$, particles with $\delta = -2.5\%$ will gain -0.13 tune shift and particles with $\delta = -2.5\%$ in a lattice with tunes below 0.13 will hit integer resonance. Similar argument holds for $\delta = 2.5\%$ and fractional tunes above 0.37. This makes the converged solutions have fractional tunes in-between $[0.15, 0.35]$ (see Fig. 4. Depending on the second order chromaticity, the exact number varies for different lattices).

A post processing script is applied on the results of the MOEA optimizer, e.g. the green circles in Fig. 4. It runs the sextupole and quadrupole settings on more random seeds of misalignment errors to filter out the candidates which have visible dependence on random seeds.

The frequency map of one solution is shown in Fig. 5. It is for x–δ plane with fixed vertical offset $y = 1\mu m$ and uses the common definition of tunes diffusion rate

$$d\nu/dt = \log\sqrt{(d\nu_x/dt)^2 + (d\nu_y/dt)^2} \qquad (3)$$

where $d\nu_x/dt = (\nu_{x,1025\to2048} - \nu_{x,1\to1024})/1024$ and $d\nu_y/dt = (\nu_{y,1025\to2048} - \nu_{y,1\to1024})/1024$ are tunes drift per turn after 1024 turns. For high precision of frequency drift, e.g. 10^{-7}, NAFF is used on 1024 turns of orbit [10].

The solution shown in Fig. 5 has a working point $(33.24, 16.36)$. Compared with tunes $(33.15, 16.27)$ optimized at lower chromaticities, the new working point stays

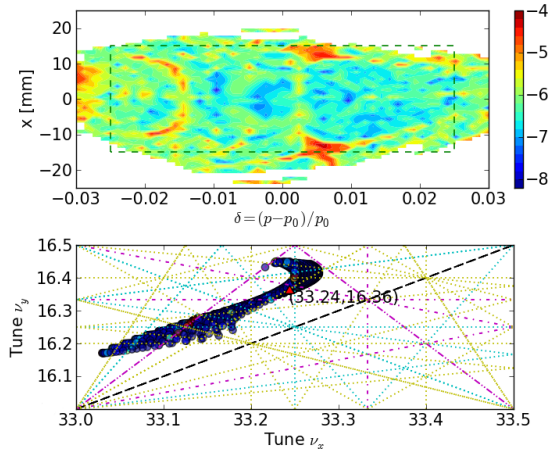

Figure 5: Frequency map and tune footprint of a candidate lattice with tunes $(33.24, 16.36)$ and fitted chromaticity $(5, 5)$.

further away from the main resonance at chromaticities $(5, 5)$. This broader range of searching is an advantage of including tunes as variables.

ACKNOWLEDGMENTS

We thank J. Bengtsson for his help on driving terms calculation, T. Tanabe for the kickmap of the damping wiggler, and M. Borland, L. Emery, D. Robin, C. Steier for fruitful discussions. This work was supported by Brookhaven Science Associates, LLC under Contract No. DE-AC02-98CH10886 with the Department of Energy.

REFERENCES

[1] W. Guo, S. Krinsky, L. Yang, "NSLS-II Lattice Optimization with Non-zero Chromaticity", IPAC'10, 2010, Kyoto, Japan.

[2] NSLS-II preliminary design report, http://www.bnl.gov/nsls2/project/PDR/

[3] L. Yang, "48th ICFA Beam Dynamic Workshop on FLS", SLAC

[4] M. Borland, ibid.

[5] SLS Note 9/97, PSI, 1997. National Accelerator Laboratory, California, March 2010.

[6] K. Deb, "Multi-Objective Optimization Using Evolutionary Algorithms", Wiley, 2001.

[7] K. Deb, Computer Methods in Applied Mechanics and Engineering 186, 311, 2000.

[8] L. Yang, D. Robin, F. Sannibale, C. Steier, and W. Wan, Nuclear Instruments and Methods in Physics Research Section A 609, 50, 2009.

[9] L. Yang, "Tracking Code Developement for Beam Dynamics Optimization", PAC'11, New York, 2011

[10] J. Laskar, C. Froeschl, A. Celletti, Physica D: Nonlinear Phenomena 56, 253, 1992